Bioorganic & Medicinal Chemistry 21 (2013) 523–531

Contents lists available at SciVerse ScienceDirect

Bioorganic & Medicinal Chemistry

journal homepage: www.elsevier.com/locate/bmc

Synthesis and anti-inflammatory evaluations of β-lapachone derivatives

Chih-Hua Tseng [a,†], Chih-Mei Cheng [b,†], Cherng-Chyi Tzeng [a], Shin-I Peng [a], Chiao-Li Yang [a], Yeh-Long Chen [a,*]

[a] Department of Medicinal and Applied Chemistry, College of Life Science, Kaohsiung Medical University, Kaohsiung City 807, Taiwan
[b] Department of Biomedical Science and Environmental Biology, College of Life Science, Kaohsiung Medical University, Kaohsiung City 807, Taiwan

ARTICLE INFO

Article history:
Received 8 October 2012
Revised 29 October 2012
Accepted 31 October 2012
Available online 24 November 2012

Keywords:
β-Lapachone (β-LAPA)
Anti-inflammatory activity
iNOS
COX-2
NO
TNF-α

ABSTRACT

β-Lapachone (β-LAPA), a natural product from the lapacho tree in South America, is a potential chemotherapeutic agent that exhibit a wide variety of pharmacological effects such as anti-virus, anti-parasitic, anti-cancer, and anti-inflammatory activities. In order to discover novel anti-inflammatory agents, we have synthesized a series of β-LAPA derivatives for evaluation. Among them, 4-(4-methoxyphenoxy) naphthalene-1,2-dione (**6b**) was found to be able to inhibit NO and TNF-α released in LPS-induced Raw 264.7 cells. Inhibition of iNOS and COX-2 was also observed in compound **6b** treated cells. Mechanism studies indicated that **6b** exhibited anti-inflammatory properties by suppressing the release of pro-inflammatory factors through down-regulating NF-κB activation. In addition, it suppressed NF-κB translocation by inhibiting the phosphorylation of p38 kinase. Our results also indicate that the inhibitory effect of **6b** on LPS-stimulated inflammatory mediator production in Raw 264.7 cell is associated with the suppression of the NF-κB and MAPK signaling pathways. A low cytotoxicity (IC_{50} = 31.70 μM) and the potent anti-inflammatory activity exhibited by compound **6b** make this compound a potential lead for developing new anti-inflammatory agents. Further structural optimization of compound **6b** is on-going.

1. Introduction

Inflammation is a central feature of many pathophysiological conditions in response to tissue injury and host defenses against microbial challenge. Pro-inflammatory cells, mainly activated macrophages, mediate most of the cellular and molecular pathophysiology of inflammation by producing cytokines and other pro-inflammatory molecules, including prostaglandins, enzymes, and free radicals such as NO.[1,2] Three isoforms of NOS exist, constitutively expressed neuronal NOS (nNOS), endothelial NOS (eNOS), and inducible isoform (iNOS).[3] Activated macrophages transcriptionally express inducible nitric oxide synthase (iNOS), which is responsible for the prolonged and profound production of NO.[4–6] The aberrant release of NO can lead to amplification of inflammation as well as tissue injury.[7] Therefore, inhibition of neutrophils and/or macrophages activation and the following release of inflammatory mediators provide a promising strategy for the development of potential anti-inflammatory agents.

Many efforts had been devoted to the discovery of novel anti-inflammatory agents for the past few years.[8–13] The natural quinones include lapachol, α-lapachone and β-lapachone (β-LAPA) (Fig. 1) were isolated from the heartwood of the Bignoniaceae family (*Tabebuia* sp) and evaluated for their biological activities. Among them, β-LAPA was found to be able to inhibit the expression of nitric oxide (NO) and PGE_2 in alveolar macrophages.[14] In order to discover novel drug candidates, we have synthesized certain furo[3′,2′:3,4]naphtho[1,2-*d*]imidazole derivatives and evaluated for their anti-inflammatory activities. Our results indicated that (*E*)-2-(2-(5-nitrofuran-2-yl)vinyl)furo[3′,2′:3,4]naphtho[1,2-*d*]imidazole (**1**) was capable of inhibiting iNOS expression, with an IC_{50} value of 0.52 μM while 2-(4-methoxyphenyl)-furo[3′,2′:3,4] naphtho[1,2-*d*]imidazole (**2**) exhibited a strongly inhibitory activity on LPS-induced PGE_2 production, with an IC_{50} value of 0.047 μM.[15,16] We have also demonstrated that certain quinolin-2(1*H*)-one derivatives such as (*E*)-4-[2-cyclohex-2-enylidene]hydrazinyl]quinolin-2(1*H*)-one (**3**) significantly suppressed LPS-induced NO production and iNOS gene expression in macrophages.[17] The present study intends to explore novel β-LAPA derivatives which possess significant anti-inflammatory potency and lower cytotoxicity. In addition to the quinone (naphthalene-1,2-dione) pharmacophores, their hydroxylamine-condensed derivatives have also been synthesized and evaluated on the ground that many hydroxylamine-condensed derivatives exhibited more potent biological activities than that of their respective ketone precursors.[18–21]

* Corresponding author. Tel.: +886 7 3121101x2684; fax: +886 7 3125339.
E-mail address: yeloch@kmu.edu.tw (Y.-L. Chen).
† These two authors contributed equally to this work.

0968-0896/$ - see front matter © 2012 Elsevier Ltd. All rights reserved.
http://dx.doi.org/10.1016/j.bmc.2012.10.047

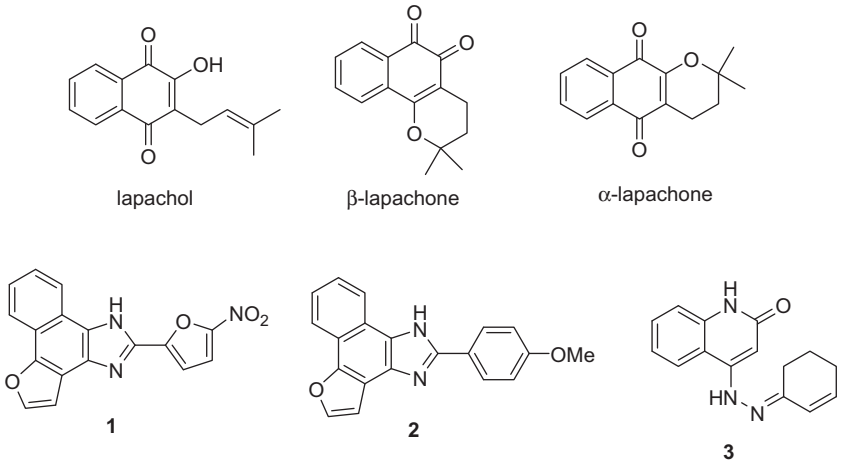

Figure 1. Structures of lapachol, β-lapachone, α-lapachone, and compounds **1**–**3**.

2. Results and discussion

2.1. Chemistry

Treatment of sodium 3,4-dioxo-3,4-dihydronaphthalene-1-sulfonate (**4**) with aniline afforded 4-(phenylamino)naphthalene-1,2-dione (**5a**) in 81% yield as described in Figure 2. The ^{1}H NMR spectrum of compound **5a** showed a total of 11 proton signals, which included ten aromatic methynes (δ_H 5.87 (3-H), 7.29–7.33 (3 Ar-H), 7.49–7.53 (2 Ar-HH), 7.75 (7-H), 7.87 (6-H), 8.05 (5-H), 8.33 (8-H)) and one broad amino-proton (δ_H 9.89), and the ^{13}C NMR spectrum of **5a** showed two carbonyl carbons (δ_C 175.92, 181.08). A correlation between δ_C 100.41/δ_H 5.87 was also observed in the HMQC spectrum of compound **5a**. Condensation of **5a** with NH_2OH gave (*Z*)-1-hydroxyimino-4-(phenylamino)naphthalene-1,2-dione (**7a**)[22] exclusively based on the spectra data. The ^{1}H NMR spectrum of compound **7a** indicated ten aromatic methynes (δ_H 5.62 (3-H), 7.40–7.44 (3 Ar-H), 7.54–7.58 (2 Ar-HH), 7.68–7.74 (6- and 7-H), 8.24 (5-H), 8.38 (8-H)), one broad amino-proton (δ_H 10.31), and one sharp oxime-proton (δ_H 18.53), and the ^{13}C NMR spectrum of **7a** showed one carbonyl carbons (δ_C 178.04) and one oxime carbon (δ_C 143.66, it was shifted upfield compared to **5a**). The HMQC spectrum of compound **7a** showed that the resonance of 3-H (δ_C 97.41/δ_H 5.62) was shifted upfield compared to that of 3-H of **5a** (δ_C 100.41/δ_H 5.87). Further, the extremely deshielded NOH proton (δ_H 18.53) can be explained by it being involved in a strong intramolecular hydrong bond to the naphthalen-2-one C=O unit. This configurational fixation is also confirmed by X-ray crystallographical analysis (Fig. 3) of compound **7a**[23], the yellow single crystal ($0.12 \times 0.08 \times 0.04$ mm^3) of **7a** was obtained by slow evaporation from MeOH/CH_2Cl_2 (10/90) solution. In the crystal structure, **7a** has a strong hydrogen bond (O(2)-H...O(1) = 1.743 Å) between (*Z*)-configurational oxime group and the C=O unit.

Accordingly, (*Z*)-1-hydroxyimino-4-(methoxyphenylamino) naphthalene-1,2-dione (**7b**) was prepared by the condensation of NH_2OH with 4-(4-methoxyphenylamino)-naphthalene-1,2-dione (**5b**) which in turn was obtained by the treatment of **4** and 4-methoxyaniline. Treatment of **4** with phenol under basic condition afforded 4-phenoxynaphthalene-1,2-dione (**6a**) in 48% yield. 4-(4-Methoxyphenoxy)-naphthalene-1,2-dione (**6b**) was obtained in a moderate yield by the treatment of **4** with 4-methoxyphenol

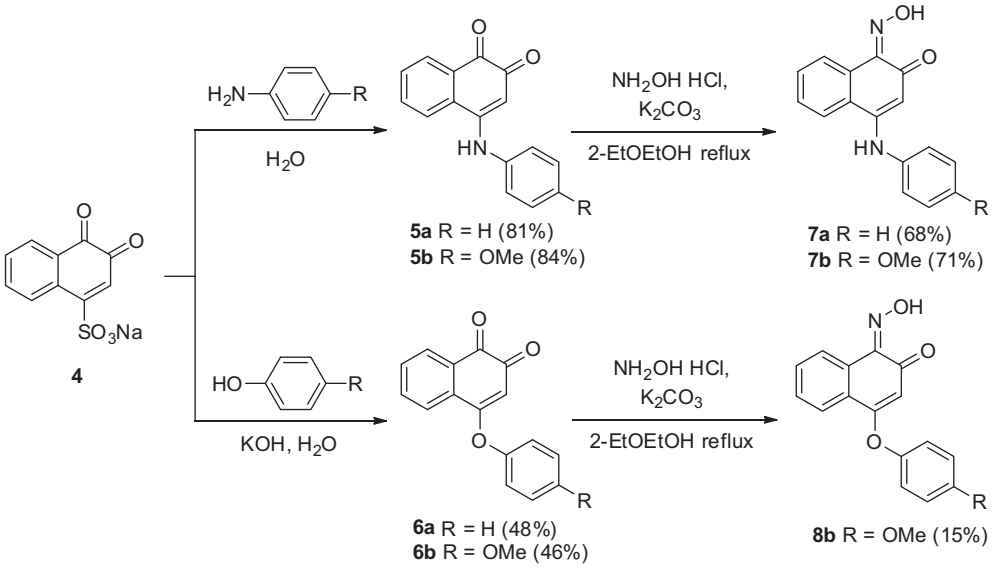

Figure 2. Synthesis of compounds **5a**–**8b**.

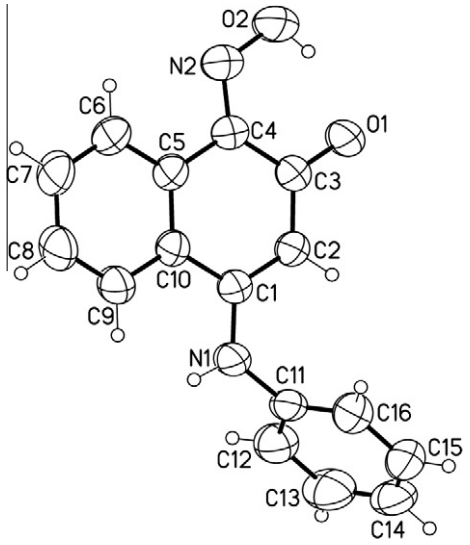

Figure 3. ORTEP view of (*Z*)-1-(hydroxyimino)-4-(phenylamino)naphthalen-2(1*H*)-one (**7a**).

under the same reaction conditions. Hydroxylamine fails to give definite products with **6a**, but condenses with **6b** gave (*Z*)-1-hydroxyimino-4-(methoxyphenoxy)naphthalene-1,2-dione (**8b**) as a sole product with low yield.

2.2. Lipopolysaccharide (LPS)-induced nitric oxide production

Murine macrophage Raw 264.7 was treated with LPS (0.1 μg/mL) for 24 h to induce NO production. The accumulation of nitrite, a stable NO metabolite was assessed by Griess reaction. Results from Table 1 indicated 4-(4-methoxyphenylamino)naphthalene-1,2-dione (**5b**) was approximately twofold less active than β-LAPA in the suppression of LPS-induced NO production. Replacement of 4-(4-methoxyphenylamino) moiety with its isosteric 4-(4-methoxyphenoxy) counterpart did not affect the inhibitory activity in which both **5b** and **6b** were able to suppress LPS-induced NO production with an IC_{50} value of 0.81 and 0.74 μM, respectively. A comparable activity was observed for **5b** and its 1-hydroxyimino derivative **7b**, while the 1-hydroxyimino derivative **8b** was less active than its parent dioxo precursor **6b**.

To identify active potential drug candidates with low cytotoxicity, Raw 264.7 cells were treated with these newly synthesized compounds and β-LAPA, respectively for 24 h. Cytotoxicity was determined by MTS assay and the results indicated that 4-phenylamino derivatives **5b**, **7a**, and **7b** were highly cytotoxic with an IC_{50} value of 1.84, 1.67, and 4.69 μM, respectively while 4-phenoxy derivatives **6a**, **6b**, and **8b** were less cytotoxic with an IC_{50} value of 28.47, 31.70, and 20.63 μM, respectively. Therefore, compounds **6a**, **6b**, and **8b** were selected for further pharmacological evaluations.

Table 1
Cytotoxicity and the inhibitory effect of β-lapachone (β-LAPA) derivatives on the accumulation of nitric oxide induced by LPS in the culture media of RAW 264.7 cells

Compound	NO inhibition IC_{50} (μM)	Cytotoxicity IC_{50} (μM)
5b	0.81 ± 0.11	1.84 ± 0.08
6a	0.85 ± 0.55	28.47 ± 3.61
6b	0.74 ± 0.16	31.70 ± 2.65
7a	0.63 ± 0.20	1.67 ± 0.13
7b	0.87 ± 0.05	4.69 ± 0.30
8b	1.29 ± 0.05	20.63 ± 2.31
β-LAPA	0.47 ± 0.04	4.06 ± 0.03
1400 W	0.20 ± 0.02	47.47 ± 1.89

2.3. Nitric oxide (NO)-scavenging effects

NO-scavenging effects of compounds **6a**, **6b**, and **8b** were measured as previously described.[24] Sodium nitroprusside (SNP) (2.5 mM) was incubated alone or in combination with tested compounds (10 μM) or 1400 W (10 μM) in light at room temperature for 60 min. Results of Figure 4 indicated the co-incubation of SNP with compound **6a**, **6b**, **8b**, β-LAPA or 1400 W did not affect the levels of nitrite.

2.4. Lipopolysaccharide (LPS)-induced iNOS and/or COX-2 protein

To address whether the inhibition of NO production was associated with decreased levels of iNOS and/or COX-2, we performed RT-PCR and Western blot analysis for detection of protein levels. Raw 264.7 cells were treated with compound **6a**, **6b**, and **8b** (0.5 μM), respectively for 24 h. The protein levels of iNOS and COX-2 were detected in whole cell lysates 24 h after LPS treatment. In iNOS protein level, three compounds were approximately equally potent in the inhibition of iNOS expression while β-LAPA and 1400 W were less active (Fig. 5A). It was clear that the density ratio of LPS-induced iNOS was significantly ($^{*}P$ <0.05 and $^{**}P$ <0.01) inhibited in a dose-dependent manner by **6b** and β-LAPA, respectively in the quantitative determination. Both compounds were found to be more active than 1400 W at a concentration of 2.0 μM (Fig. 5B). Therefore, our results indicated the inhibition of NO production by **6b** and β-LAPA was associated at least partly with decreased levels of iNOS. Results had also indicated the inhibition of NO production by 1400 W may not be associated with decreased levels of iNOS.

As shown in Figure 5C, the LPS induced COX-2 level was significantly inhibit by all the compounds tested and the inhibitory activity decreased in an order of **6b** > **6a** > **8b** at 0.5 μM. Compound **6b** was approximately equal potent with 1400 W and was more active than β-LAPA at a concentration of 0.5 μM. Compound **6b** and β-LAPA were found to inhibited the LPS induced COX-2 level in a dose-dependent manner as shown in Figure 5D. The inhibitory activity decreased in an order of **6b** > β-LAPA > 1400 W at 2.0 μM. Therefore, our results indicated that the inhibition of NO production by **6b** and β-LAPA was associated at least partly with decreased levels of COX-2.

2.5. Lipopolysaccharide (LPS)-induced iNOS mRNA

Compound **6b** was proved to be able to suppress LPS-induced NO production through the inhibition of iNOS and COX-2 levels.

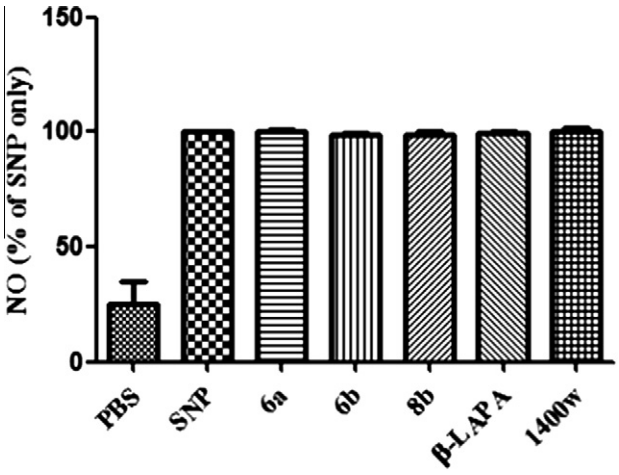

Figure 4. NO-scavenging effects of 1400 W, β-LAPA, compounds **6a**, **6b**, and **8b**. SNP solution (2.5 mM) in PBS was incubated alone or with tested compound (10 μM) or 1400 W (10 μM) in the presence of light at room temperature for 60 min.

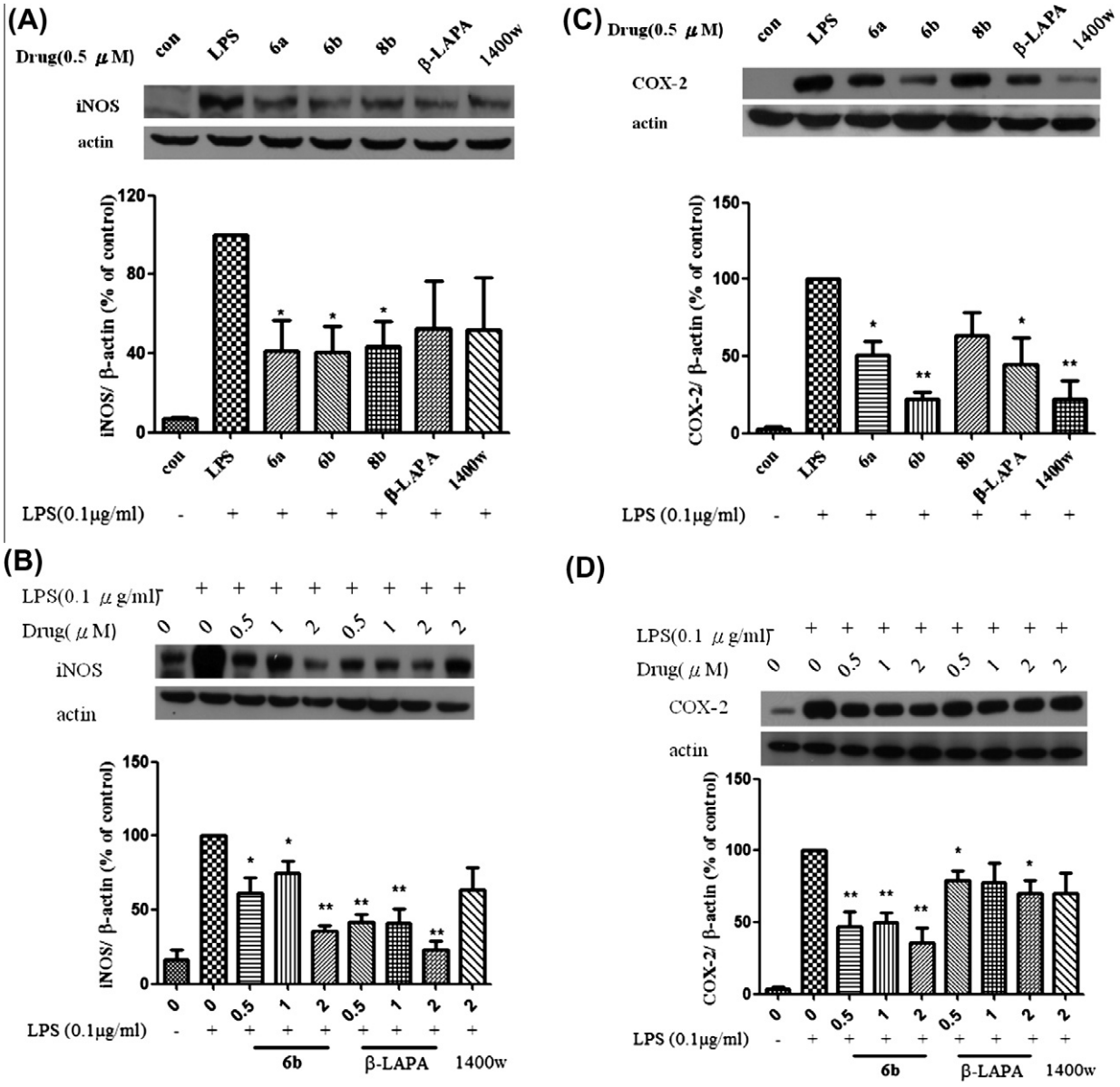

Figure 5. Inhibition of iNOS and COX-2 expression by β-LAPA analogues and 1400 W in LPS-stimulated RAW 264.7 cells. Cells (5×10^5 cells/well) were pretreated with the indicated concentrations of tested compounds for 2 h before incubation with 0.1 μg/mL LPS for 24 h. Cell lysates were then prepared and Western blots were performed using an antibody specific for murine iNOS (A, B) and COX-2 (C, D). Data are presented as means + S.D. mean of 3 separate experiments performed in triplicate. $^{*}P$ <0.05 as compared with control. $^{**}P$ <0.01 as compared with LPS alone.

We further investigated whether the inhibition of NO production was associated with decreased levels of iNOS mRNA. As shown in Figure 6, iNOS mRNA level was significantly decreased by **6b** and β-LAPA in a dose-dependent manner for 9 h after LPS treatment. The inhibitory activity decreased in an order of **6b** > β-LAPA > 1400 W at 2.0 μM.

2.6. Lipopolysaccharide (LPS)-induced TNF-α production

To determine the effect of β-LAPA derivatives in the production of pro-inflammatory cytokine TNF-α production, we have analyzed the effects of **6b** and β-LAPA on pro-inflammatory cytokines, such as TNF-α. Raw 264.7 cells were incubated with **6b** and β-LAPA, respectively (0.5, 1.0, 2.0, or 5.0 μM) in the presence or absence of LPS (0.1 μg/mL) for 24 h, and cytokine levels in the culture medium were measured. As shown in Figure 7A, TNF-α level was significantly decreased by **6b** and β-LAPA in a concentration-dependent manner, and compound **6b** was more active than β-LAPA at the same concentrations. These results indicated that reduced expression of iNOS and COX-2 by **6b** and β-LAPA were liable for inhibition of NO and TNF-α production.

2.7. Lipopolysaccharide (LPS)-induced MMP-9 expression

To determine whether compound **6b** and β-LAPA affect the activity of MMP-9 in LPS-stimulated macrophages, Raw 264.7 cells were incubated with different concentrations of **6b** and β-LAPA, respectively, followed by stimulation with LPS as described above and the activity of MMP-9 was analyzed by gelatin zymography. We found the activity of MMP-9 was significantly inhibited by the treatment of **6b** and β-LAPA in a dose dependent manner (Fig. 7B).

2.8. Effect of 6b on NF-κB activity

NF-κB is a primary regulator of genes that are involved in the production of pro-inflammatory cytokines and enzymes involved

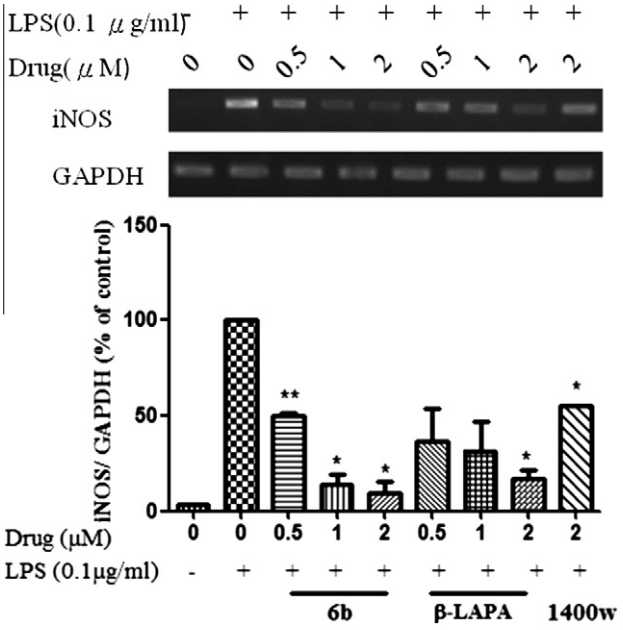

Figure 6. Inhibitory effects of compound **6b** on LPS-induced iNOS mRNA expression. Cells (5×10^5 cells/well) were pretreated with the indicated concentrations of tested compounds for 2 h before incubation with 0.1 μg/mL LPS for 9 h. Total RNA was prepared for RT-PCR analysis of iNOS mRNA expression in LPS-stimulated RAW 264.7 cells. GAPDH were used as internal controls for the RT-PCR assays. Data are presented as means + S.D. mean of 3 separate experiments performed in triplicate. $^{*}P$ <0.05 as compared with control. $^{**}P$ <0.01 as compared with LPS alone.

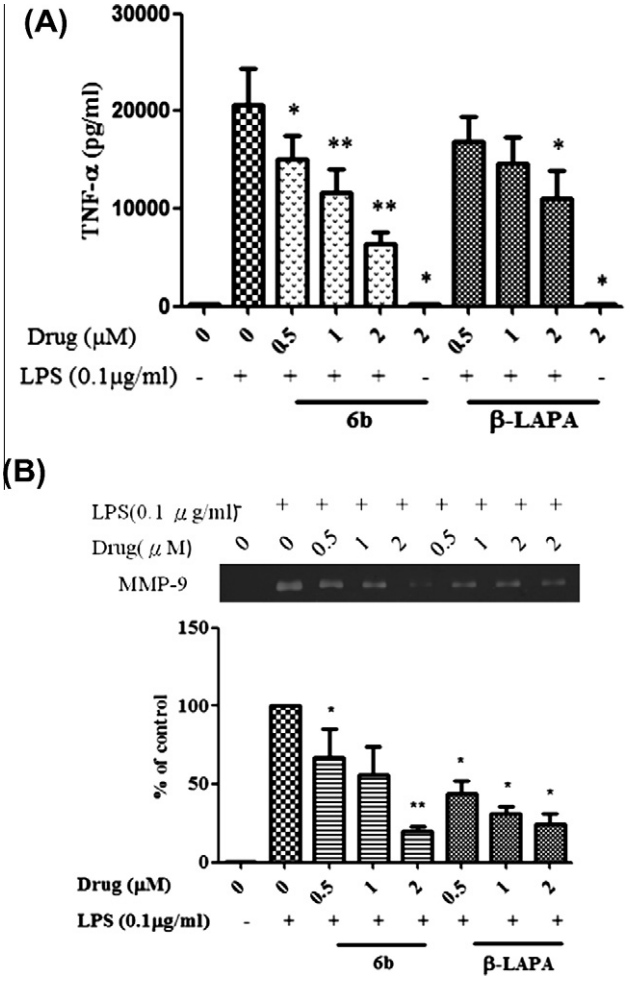

Figure 7. Inhibitory effects of compound **6b** on LPS-induced TNF-α, and MMP-9 expression. Cells (5×10^5 cells/well) were pretreated with the indicated concentrations of tested compounds for 2 h before incubation with 0.1 μg/mL LPS for 24 h. The amounts of TNF-α were determined using ELISA in culture medium. (A) The medium was collected and used in zymography, activity was measured by scanning the zymogram, quantified the intensity of the MMP-9 band and expressed the intensity as % of control. (B) Data are presented as means + S.D. mean of 3 separate experiments performed in triplicate. $^{*}P$ <0.05 as compared with control. $^{**}P$ <0.01 as compared with LPS alone.

in the inflammatory process.[25] To clarify the influence of **6b** on NF-κB p65 nuclear translocation, the nuclear localization of NF-κB in Raw 264.7 cells was analyzed using laser confocal immunofluorescent microscopy (Fig. 8). The confocal images revealed that NF-κB p65 was normally sequestered in the cytoplasm, and that nuclear localization of NF-κB p65was significantly induced after stimulation of cells with LPS. The LPS-induced translocation of NF-κB p65 was completely abolished after pre-treating the cells with **6b**. Nuclear translocation of NF-κB p65 was not observed in the cells after pre-treatment with cordycepin alone in the absence of LPS stimulation. Taken together, these findings showed that the NF-κB pathway was involved in the anti-inflammatory effect of **6b** in LPS-stimulated Raw 264.7 cells.

2.9. Effects of 6b and β-LAPA on the phosphorylation of p-38 kinase in LPS-stimulated Raw 264.7 cells

The MAPK pathways are known to be important for the expression of iNOS and COX-2.[26] Therefore, MAP kinases act as specific targets for inflammatory responses. To test whether the inhibition of inflammation by cordycepin is regulated through the MAP kinase pathways, we examined the effect of **6b** and β-LAPA on LPS-induced phosphorylation of p38 kinase in Raw 264.7 cells using Western blot analysis. As shown in Figure 9, **6b** and β-LAPA attenuated the LPS-stimulated phosphorylation of p38 in a concentration-dependent manner. In contrast, the amounts of p38 kinase were unaffected by either LPS or **6b** treatment. These results suggested that the MAPK pathways were involved during LPS-mediated expression of inflammatory mediators.

3. Conclusion

In summary, we have synthesized certain β-LAPA derivatives and evaluated for their anti-inflammatory activities. Results indicated that 4-(4-methoxyphenoxy)-naphthalene-1,2-dione (**6b**) and β-LAPA significantly attenuated the release of inflammatory mediators (NO and TNF-α, MMP-9) in a concentration-dependent manner. These data indicated that **6b** and β-LAPA target p38 kinase and NF-κB. These compounds inhibit iNOS, COX-2, and the formation of pro-inflammatory cytokine NO, TNF-α, MMP-9. Although β-LAPA was able to suppress LPS-induced NO production with an IC_{50} value of 0.47 μM, its high cytotoxicity against the growth of RAW 264.7 cells with an IC_{50} value of 4.06 μM limited its further development as a potential drug candidate. We have identified a new type of β-LAPA derivatives which are non cytotoxic and exhibited the same anti-inflammatory mechanism with β-LAPA. Among them, **6b** may serve as a new lead for the discovery of potential anti-inflammatory agents.

4. Experimental part

4.1. General

TLC: Precoated (0.2 mm) silica gel 60 F_{254} plates from EM Laboratories, Inc.; detection by UV light (254 nm). Mp: electrothermal IA9100 digital melting-point apparatus; uncorrected. The

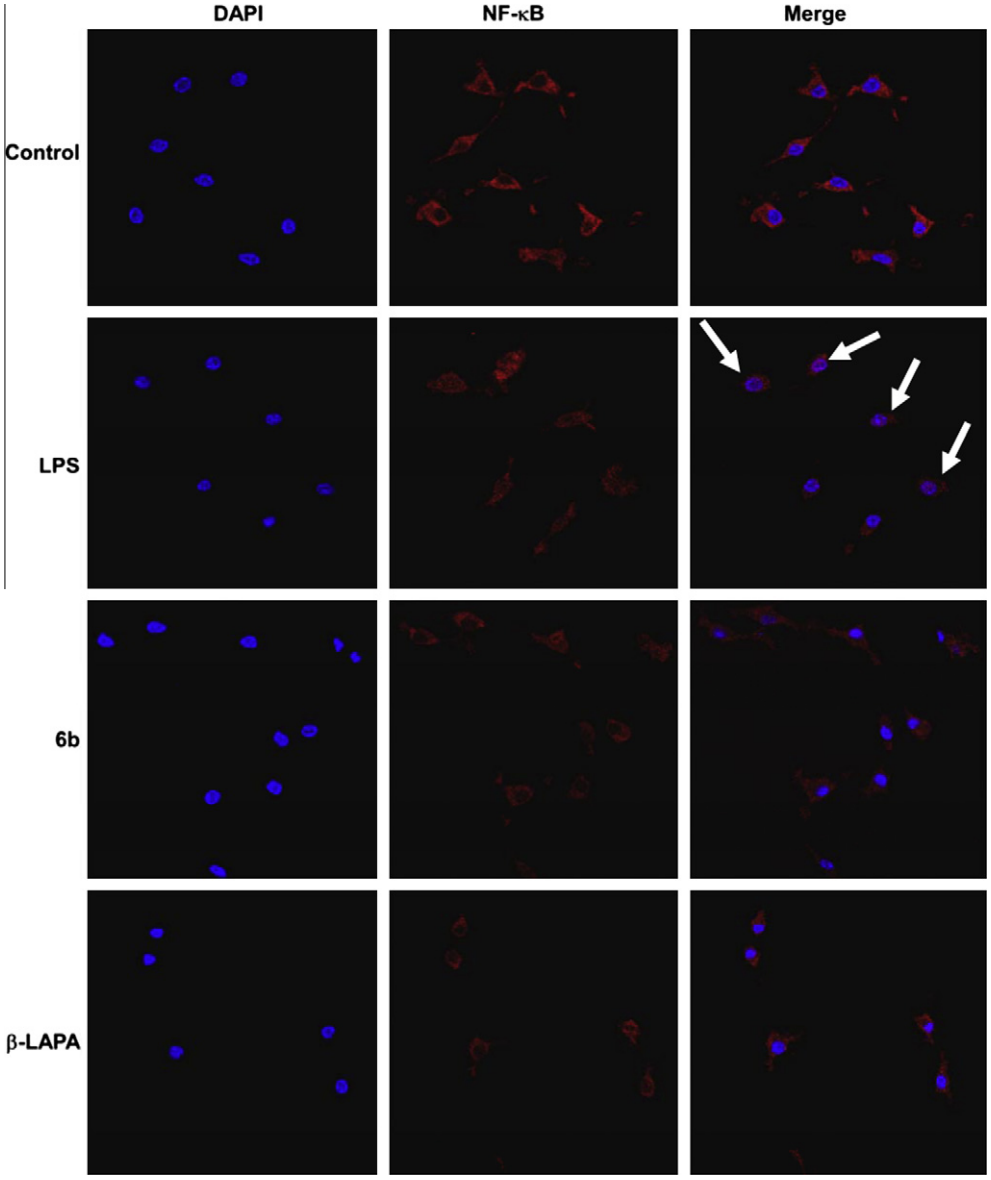

Figure 8. Effects of **6b** on NF-κB activity in LPS-stimulated RAW 264.7 cell. Localization of NF-κB p65 was visualized with fluorescence microscopy after immunofluorescence staining with NF-κB p65 antibody (red). Cells were stained with DAPI for visualization of nuclei (blue). White arrows indicate the nuclear localization of NF-kB.

ultraviolet–visible (UV–VIS) absorption spectra were recorded on a Jasco V570 spectrometer. IR spectra were measured on PERKIN ELMER System 2000 FT-IR spectrophotometer. ^{1}H and ^{13}C NMR spectra: Varian-Unity-400 spectrometer at 400 and 100 MHz or Varian-Gemini-200 spectrometer at 200 and 50 MHz, chemical shifts δ in ppm with $SiMe_4$ as an internal standard (=0 ppm), coupling constants J in Hz. Elemental analyses were carried out on a Heraeus CHN–O-Rapid elemental analyzer, and results were within ±0.4% of calculated values.

4.1.1. 4-(Phenylamino)naphthalene-1,2-dione (5a)

To a solution of sodium 3,4-dioxo-3,4-dihydronaphthalene-1-sulfonate (**4**) (1.30 g, 5.0 mmol) in water (150 mL) was added aniline (0.48 g, 5.5 mmol). The reaction mixture was stirred at room temperature for 20 min (TLC monitoring). The solvent was removed in vacuo and the resulting residue was crystallized from EtOH to give 1.10 g (81%) of **5a** as a red solid. Mp: 272–274 °C. UV λ_{max} nm ($\log\varepsilon$): 460 (3.73), 278 (4.22), 243 (4.41), 206 (4.21) in MeOH. IR (KBr pellets) cm^{-1}: 3318, 1583, 1520. ^{1}H NMR (400 MHz, $CDCl_3$): 5.87 (br s, 1H, 3-H), 7.29–7.33 (m, 3H, Ar-H), 7.49–7.53 (m, 2H, Ar-H), 7.73–7.77 (m, 1H, 7-H), 7.86–7.89 (m, 1H, 6-H), 8.05 (d, 1H, J = 7.6 Hz 5-H), 8.33 (d, 1H, J = 8.0 Hz, 8-H), 9.89 (br s, 1H, NH). ^{13}C NMR (100 MHz, $CDCl_3$): 100.41, 103.73, 120.00, 123.98, 126.01, 126.84, 128.19, 129.42 (2C), 131.52 (2C), 134.32, 137.87, 154.64, 175.92, 181.08. Anal. calcd for $C_{16}H_{11}NO_2$: C 77.10, H 4.45, N 5.62; found: C 77.01, H 4.70, N 5.41.

4.1.2. 4-(4-Methoxyphenylamino)naphthalene-1,2-dione (5b)

From **4** as described for **5a**, to give of **5b** as a brown solid (1.13 g, 84% yield). Mp: 108–110 °C. UV λ_{max} nm ($\log\varepsilon$): 429 (3.51), 278 (4.17), 225 (4.34), 204(3.93) in MeOH. IR (KBr pellets) cm^{-1}: 3328, 1582, 1522. ^{1}H NMR (400 MHz, DMSO-d_6): 3.83 (s, 3H, OMe), 5.63 (s, 1H, 3-H), 7.04–7.07 (m, 2H, Ar-H), 7.26–7.29 (m, 2H, Ar-H), 7.68–7.72 (m, 1H, 7-H), 7.80–7.82 (m, 1H, 6-H), 8.05 (d, 1H, J = 7.6 Hz, 5-H), 8.30 (d, 1H, J = 8.0 Hz, 8-H), 9.80 (br s, 1H, NH). ^{13}C NMR (100 MHz, DMSO-d_6): 55.16, 99.96, 104.38, 114.40 (2C), 123.58, 125.58, 127.33 (2C), 127.93, 130.11, 131.12, 133.97,

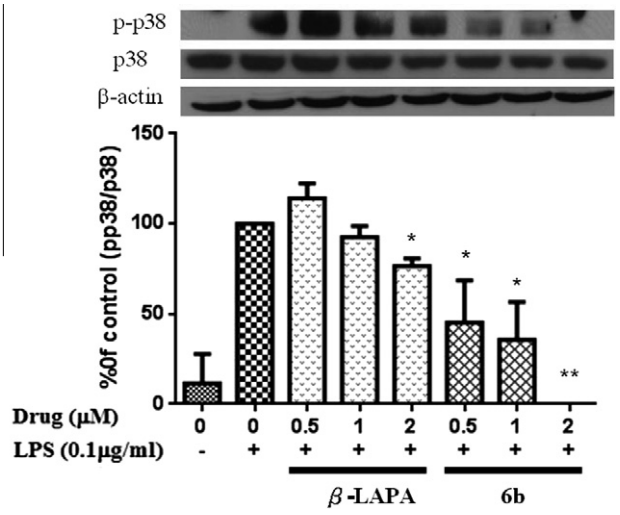

Figure 9. Inhibitory effects of compounds **6b** on LPS-induced p-p38 protein expression. Cells (5×10^5 cells/well) were pretreated with the indicated concentrations of tested compounds for 2 h before incubation with 0.1 μg/mL LPS for 24 h. Proteins (15 μg) of total cell lysates were separated by 8% SDS–PAGE, p38 and p-p38 protein expression was detected by Western blot and analyzed by densitometry. The relative density was calculated as the ratio of p-p38 expression to β-actin expression. Data are presented as means + S.D.mean of 3 separate experiments performed in triplicate. *P<0.05 as compared with control. **P<0.01 as compared with LPS alone.

154.97, 157.90, 175.55, 181.31. Anal. calcd for $C_{17}H_{13}NO_3$: C 73.11, H 4.69, N 5.02; found: C 72.92, H 4.81, N 5.05.

4.1.3. 4-Phenoxynaphthalene-1,2-dione (6a)

To a solution of **4** (1.30 g, 5.0 mmol) in water (150 mL) was added phenol (0.47 g, 5.5 mmol) and potassium hydroxide (0.28 g, 5.0 mmol). The reaction mixture was stirred at room temperature for 20 min (TLC monitoring). The solvent was removed in vacuo and the resulting residue was crystallized from EtOH to give 0.62 g (48%) of **6a** as a yellow solid. Mp: 163–165 °C. UV λ_{max} nm ($\log\varepsilon$): 401 (3.24), 251 (4.38), 218 (4.47) in MeOH. IR (KBr pellets) cm^{-1}: 1646, 1564, 1363, 1231. ^1H NMR (400 MHz, $CDCl_3$): 5.67 (s, 1H, 3-H), 7.15–7.19 (m, 2H, Ar-H), 7.34–7.38 (m, 1H, Ar-H), 7.47–7.52 (m, 2H, Ar-H), 7.67 (td, 1H, *J* = 7.6, 1.2 Hz, 7-H), 7.79 (td, 1H, *J* = 7.6, 1.6 Hz, 6-H), 8.10 (dd, 1H, *J* = 7.6, 1.2 Hz, 5-H), 8.18 (dd, 1H, *J* = 7.6, 1.6 Hz, 8-H). ^{13}C NMR (100 MHz, $CDCl_3$): 106.40, 121.28 (2C), 124.90, 126.95, 129.41, 130.39 (2C), 130.49, 131.63, 131.91, 135.12, 152.33, 168.81, 179.29, 179.55. Anal. calcd for $C_{16}H_{10}O_3 \cdot 0.3H_2O$: C 75.17, H 4.18; found: C 75.16, H 4.19.

4.1.4. 4-(4-Methoxyphenoxy)naphthalene-1,2-dione (6b)

From **4** as described for **6a**, to give 0.64 g (46%) of **6b** as a yellow solid. Mp: 174–175 °C. UV λ_{max} nm ($\log\varepsilon$): 338 (3.46), 250 (4.39), 224 (4.55) in MeOH. IR (KBr pellets) cm^{-1}: 1649, 1563, 1363, 1193. ^1H NMR (400 MHz, $CDCl_3$): 3.84 (s, 3H, OMe), 5.67 (s, 1H, 3-H), 6.95–6.99 (m, 2H, Ar-H), 7.05–7.09 (m, 2H, Ar-H), 7.65 (td, 1H, *J* = 7.6, 1.2 Hz, 7-H), 7.77 (td, 1H, *J* = 7.6, 1.2 Hz, 6-H), 8.08 (dd, 1H, *J* = 8.0, 1.2 Hz, 8-H), 8.16 (dd, 1H, *J* = 7.6, 1.2 Hz, 5-H). ^{13}C NMR (100 MHz, $CDCl_3$): 55.74, 106.24, 115.28(2C), 122.10 (2C), 124.89 (2C), 129.36, 130.47, 131.69, 131.85, 135.10, 145.67, 158.06, 169.28, 179.40, 179.56. Anal. calcd for $C_{17}H_{12}O_4$: C 72.84, H 4.32; found: C 72.84, H 4.34.

4.1.5. (*Z*)-1-(Hydroxyimino)-4-(phenylamino)naphthalen-2(1*H*)-one (7a)

A mixture of **5a** (0.50 g, 2.0 mmol), hydroxylamine·HCl (0.16 g, 2.2 mmol), potassium carbonate (0.56 g, 4.0 mmol), and 2-ethoxyethanol (10 mL) was heated at reflux for 3 h (TLC monitoring). The solvent was removed in vacuo and the residue was suspended in H_2O (20 mL). The resulting precipitate that separated was collected, washed with H_2O, and dried to give a crude solid. The crude product was crystallized from EtOH to afford **7a** as a red solid (0.32 g, 68%). Mp: 226–228 °C. UV λ_{max} nm ($\log\varepsilon$): 411 (3.88), 340 (4.08), 269 (4.10), 214 (4.32) in MeOH. IR (KBr pellets) cm^{-1}: 3443, 3303, 1592, 1517. ^1H NMR (400 MHz, DMSO-d_6): 5.62 (s, 1H, 3-H), 7.40–7.44 (m, 3H, Ar-H), 7.54–7.58 (m, 2H, Ar-H), 7.68–7.74 (m, 2H, 6- and 7-H), 8.26–8.30 (m, 1H, 5-H), 8.36–8.40 (m, 1H, 8-H), 10.31 (br s, 1H, NH), 18.53 (s, 1H, NOH). ^{13}C NMR (100 MHz, DMSO-d_6): 97.41, 122.47, 123.54, 124.02, 126.20 (2C), 127.33, 129.24, 129.67 (2C), 131.33, 131.54, 137.57, 143.66, 156.95, 178.04. Anal. calcd for $C_{16}H_{14}N_{12}O_2$: C 72.72, H 4.58, N 10.60; found: C 72.35, H 4.50, N 10.54.

4.1.6. (*Z*)-1-(Hydroxyimino)-4-(4-methoxyphenylamino)naphthalen-2(1*H*)-one (7b)

From **4** as described for **7a**, to give 0.38 g (71%) of **7b** as a red solid. Mp: 224–226°C. UV λ_{max} nm ($\log\varepsilon$): 417 (3.90), 347 (4.09), 270 (4.20), 224 (4.56) in MeOH. IR (KBr pellets) cm^{-1}: 3442, 3255, 1607, 1505. ^1H NMR (400 MHz, DMSO-d_6): δ 3.83 (s, 3H, OMe), 5.52 (s, 1H, 3-H), 7.08–7.12 (m, 2H, Ar-H), 7.32–7.36 (m, 2H, Ar-H), 7.66–7.73 (m, 2H, 6- and 7-H), 8.25–8.29 (m, 1H, 5-H), 8.35–8.39 (m, 1H, 8-H), 10.24 (br s, 1H, NH), 18.61 (s, 1H, NOH). ^{13}C NMR (100 MHz, DMSO-d_6): 55.40, 97.05, 114.81 (2C), 122.43, 123.43, 124.04, 127.64 (2C), 129.16, 130.13, 131.34, 131.44, 143.70, 157.41, 158.25, 177.65. Anal. calcd for $C_{17}H_{14}N_2O_3 \cdot 0.2H_2O$: C 68.53, H 4.87, N 9.40; found: C 68.32, H 4.82, N 9.16.

4.1.7. (*Z*)-1-(Hydroxyimino)-4-(4-methoxyphenoxy)naphthalen-2(1*H*)-one (8b)

From **6b** as described for **7b**, to give of **8b** a yellow solid (0.08 g, 15% yield). Mp: 108–110 °C. UV λ_{max} nm ($\log\varepsilon$): 429 (3.51), 278 (4.17), 225 (4.34), 204 (3.93) in MeOH. IR (KBr pellets) cm^{-1}: 3438, 1504, 1213. ^1H NMR (400 MHz, $CDCl_3$): 3.84 (s, 3H, OMe), 6.93–6.96 (m, 2H, Ar-H),7.00–7.06 (m, 2H, Ar-H), 7.26 (s, 1H, 3-H), 7.68–7.82 (m, 2H, 6- and 7-H), 8.30 (d, 1H, *J* = 8.0 Hz, 5-H), 8.55 (d, 1H, *J* = 8.0 Hz, 8-H), 12.11 (s, 1H, NOH). ^{13}C NMR (100 MHz, $CDCl_3$): 55.68, 102.61, 115.23 (2C), 120.84 (2C), 122.54, 125.25, 127.11, 127.91, 131.17, 131.47, 147.88, 149.44, 151.90, 156.50, 178.35. Anal. calcd for $C_{17}H_{13}NO_4 \cdot 0.6H_2O$: C 66.70, H 4.68, N 4.58; found: C 66.92, H 5.05, N 4.63.

4.2. Biological testing

4.2.1. Cell culture

Raw 264.7 cells, purchased from Food Industry Research and Development Institute, Taiwan, were cultured in DMEM, supplemented with 5% fetal bovine serum, 100 units/mL of penicillin, 100 μg/mL of streptomycin, 2 mM L-glutamine, and 1 mM non-essential amino acids in a 10-cm plate at a density of 1×10^6 cells/mL, at 37 °C in a humidified atmosphere containing 5% CO_2.

4.2.2. Nitrite and TNF-α measurement

Nitrite was measured by adding 100 μL of the Griess reagent[27] (1% sulfanilamide and 0.1% *N*-(1-naphthyl)ethylenediamine dihydrochloride in 5% phosphoric acid) to 100 μL of medium for 5 min. The optical density at 550 nm (OD_{550}) was measured with a microplate reader. Concentrations were calculated by comparison with the OD_{550} of a standard solution of sodium nitrite prepared in culture medium. The levels of TNF-α[28] in the RAW264.7 cell culture medium were measured by Elisa assay kits according to the manufacturer's instructions (R&D).

4.2.3. Cell viability

To evaluate whether the suppressive effect of β-lapachone derivatives on nitrite production is related to cell viability. Raw 264.7 cells were treated with LPS for 24 h, and washed with 500 μL of phosphate buffer solution (PBS) before resuspended in 1 mL of culture medium. Cell viability was assessed by the MTS[29] staining method. Briefly, cells at 5×10^4 cells/well were seeded into 96-well microtiter plates and treated with various reagents for 24 h. Twenty microliters of MTS solution was added to the cells which were then incubated at 37 °C for 1 h. Color was measured spectrophotometrically in a microtiter plate reader at 490 nm and used as a relative measure of viable cell number. The number of viable cells following treatment was compared to solvent and untreated control cells and used to determine the percent of control growth as $(Ab_{treated}/Ab_{control})\times 100$, where Ab represents the mean absorbance ($n = 3$). The concentration that killed 50% of cells (IC_{50}) was determined from the linear portion of the curve by calculating the concentration of agent that reduced absorbance in treated cells, compared to control cells, by 50%.

4.2.4. NO-scavenging activity

To understand the inhibitory effects of compounds **6a**, **6b** and **8b** on NO production, sodium nitroprusside (SNP)[24] was freshly prepared at 5 mM in PBS was incubated alone or in combination with 10 μM of the different compounds. SNP is an inorganic complex where NO is found as NO^+ and light irradiation is necessary for the release of NO. Therefore, incubation mixtures were incubated in light at room temperature, and nitrite levels were determined after 60 min by Griess reaction.

4.2.5. Western blotting

Raw 264.7 cells were pretreated with tested compound for 2 h before stimulation in the presence or absence of LPS (0.1 μg/mL). Cell were harvest and lysed with RIPA lysis buffer(50 mM Tris–Cl, pH 8.0, 150 mM NaCl, 0.1% SDS, 0.5% NP-40, 1% sodiumdeoxycholate, 1 mM phenylmethyl-sulfonylfluoride, 1 mM EDTA, no added proteinase) 24 h after treatment. The total protein in the cell lysates was assayed according to the method described by Bradford.[30] Equal amounts (20–50 μg) of protein were separated using 8–15% SDS–PAGE. Proteins were transferred to Immobilon PVDF membranes (Millipore) and subsequently blocked in 5% bovine serum albumin (BSA)–Tris-Buffered Saline Tween (TBST, 100 mM Tris, pH 8.0, 150 mM NaCl and 0.1% Tween 20) for 1 h at room temperature. Specific antibodies against iNOS, COX-2, p38 and p-p38 were diluted in 5% BSA–TBST. After incubation with the appropriate primary antibody, membranes were incubated for 1 h at room temperature with a secondary antibody conjugated to horseradish peroxidase (1:10,000 dilution; Santa Cruz Biotechnology, Santa Cruz, CA). Following three washes in TBST, immunoreactive bands were visualized using the ECL detection system (ECL Amersham).

4.2.6. Isolation of total RNA and RT-PCR

Raw 264.7 cells treated with LPS (0.1 μg/mL) in the presence or absence of drug were homogenized with 1 mL of Trizol reagent (InvitrogenTM), and total RNA was isolated according to the manufacturer's protocol. One microgram of RNA was used for the reverse transcription of first strand cDNA using the oligo dT primers. Five microliters of cDNA were used for the amplification of iNOS and GAPDH (glyceraldehyde 3-phosphate dehydrogenase) mRNA expression.[31] The primers for rat iNOS are as follows: 5′-ACT GCG TCG CTT CAT TAG GT-3′ (forward) and 5′-TAG GCA AGC GCT TTA CCA CT-3′(reverse). The primers for rat glyceraldehyde 3-phosphate dehydrogenase are as follows, forward: 5′ ATG GCA CAG TCA AGG CTG AGA-3′ reverse:5′-AGA CGC CAG TAG ACT CCA CGA C-303′. The amplicons were electrophoresed on a 3% agarose gel. The gel was then examined and band intensities were measured using a spectrophotometer (Lab work) and normalized against GAPDH.

4.2.7. Gelatin zymography

Metalloproteinase activity was assayed by gelatin zymography. Raw 264.7 cells were plated in 10 cm culture for 16–18 h before treatmentin. Cells were treated with or without LPS (0.1 μg/ml) and β-LAPA, compounds **6b** (0.5, 1.0, 2.0 μM), and culture medium was collected 24 h after initiation of the treatment. The medium was concentrated using an Amicon Ultra 4 (Millipore). Equal amount of concentrated medium was fractionated by SDS–PAGE on gelatin gel (7.5% acrylamide,2 mg/ml gelatin, Sigma). Separated protein was renatured by incubating the gel for 1 h with 2.5% Triton-X100, and then with renaturing buffer (40 mM Tris, pH 7.5, 200 mM NaCl, 10 mM $CaCl_2$) overnight at 37 °C. Finally, the gel was incubated for 16–18 h with gentle shaking at room temperature with a developing buffer containing 40 mM Tris pH 7.5, 200 mM NaCl, 10 mM $CaCl_2$. Gels were stained in 0.1% coomassie-blue (R250, Sigma) for 1 h and destained until the bands were evident.[32]

4.2.8. Immunofluorescence staining and confocal laser scanning microscopy study

The NF-κB p65 nuclear localization was detected by indirect immunofluorescence assays using confocal microscopy. Raw 264.7 cells were cultured directly on glass coverslips in 24-well plates for 24 h. After stimulation with 0.1 μg/mL of LPS and/or 0.5 μM of β-LAPA or **6b**, the cells were fixed with 4% paraformaldehyde in PBS, permeabilized with 0.2% triton X-100 in PBS. Polyclonal antibodies against anti-NF-κB p65 (Santa Cruz) (1 μg/well) were applied for 24 h, followed by an 1 h incubation with FITC-conjugated anti-mouse Alexa fluor 568 (Invitrogen). The position of the cell nucleus was determined with DAPI. After washing with PBS, the coverslips were mounted with Mounting medium (DAKO), and the fluorescence was visualized using an Olympus FluorView® FV100 laser scanning confocal microscope.[33]

4.3. Statistical analysis

The results were expressed as means ± S.D. Differences in mean values between groups were analyzed by a one-way analysis of variance (ANOVA) and Student's *t*-test. For the septic shock assay, we used the log-rank test. Statistical significance was assessed as $p < 0.05$ [$^{*}p < 0.05$; $^{**}p < 0.01$].

Acknowledgments

Financial support of this work by the *National Science Council of the Republic of China* (NSC 99-2320-B-037-0-18-MY2) is gratefully acknowledged. We also thank the *National Center for High-Performance Computing* for providing computer resources and chemical database services.

References and notes

1. Laskin, D. L.; Pendino, K. J. *Annu. Rev. Pharmacol. Toxicol.* **1995**, *35*, 655.
2. Laskin, D. L.; Laskin, J. D. *Toxicology* **2001**, *160*, 111.
3. Bian, K.; Harari, Y.; Zhong, M.; Lai, M.; Castro, G.; Weisbrodt, N.; Murad, F. *Mol. Pharmacol.* **2001**, *59*, 939.
4. Solbach, W.; Moll, H.; Röllinghoff, M. *Immunol. Today* **1991**, *12*, 4.
5. Beutler, B.; Cerami, A. *Annu. Rev. Biochem.* **1988**, *57*, 505.
6. Xie, Q.; Nathan, C. *J. Leukocyte Biol.* **1994**, *56*, 576.
7. McCartney-Francis, N.; Allen, J. B.; Mizel, D. E.; Albina, J. E.; Xie, Q. W.; Nathan, C. F.; Wahl, S. M. *J. Exp. Med.* **1993**, *178*, 749.
8. Meng, X. L.; Yang, J. Y.; Chen, G. L.; Zhang, L. J.; Wang, L. H.; Li, J.; Wang, J. M.; Wu, C. F. *Int. Immunopharmacol.* **2008**, *8*, 1074.
9. Shin, H. M.; Lee, Y. R.; Chang, Y. S.; Lee, J. Y.; Kim, B. H.; Min, K. R.; Kim, Y. *Int. Immunopharmacol.* **2006**, *6*, 916.

10. Meng, X. L.; Yang, J. Y.; Chen, G. L.; Wang, L. H.; Zhang, L. J.; Wang, S.; Li, J.; Wu, C. F. *Chem. Biol. Interact.* **2008**, *174*, 51.
11. Shin, E. M.; Zhou, H. Y.; Guo, L. Y.; Kim, J. A.; Lee, S. H.; Merfort, I.; Kang, S. S.; Kim, H. S.; Kim, S.; Kim, Y. S. *Int. Immunopharmacol.* **2008**, *8*, 1524.
12. Côté, B.; Boulet, L.; Brideau, C.; Claveau, D.; Ethier, D.; Frenette, R.; Gagnon, M.; Giroux, A.; Guay, J.; Guiral, S.; Mancini, J.; Martins, E.; Massé, F.; Méthot, N.; Riendeau, D.; Rubin, J.; Xu, D.; Yu, H.; Ducharme, Y.; Friesen, R. W. *Bioorg. Med. Chem. Lett.* **2007**, *17*, 6816.
13. Liu, F. Z.; Fang, H.; Zhu, H. W.; Wang, Q.; Yang, Y.; Xu, W. F. *Bioorg. Med. Chem.* **2008**, *16*, 578.
14. Liu, S. H.; Tzeng, H. P.; Kuo, M. L.; Lin-Shiau, S. Y. *Br. J. Pharmacol.* **1999**, *126*, 746.
15. Tseng, C. H.; Lin, C. S.; Shih, P. K.; Tsao, L. T.; Wang, J. P.; Cheng, C. M.; Tzeng, C. C.; Chen, Y. L. *Bioorg. Med. Chem.* **2009**, *17*, 6773.
16. Tseng, C. H.; Tzeng, C. C.; Shih, P. K.; Yang, C. N.; Chuang, Y. C.; Peng, S. I.; Lin, C. S.; Wang, J. P.; Cheng, C. M.; Chen, Y. L. *Mol. Diversity* **2012**, *16*, 215.
17. Lin, M. W.; Tsao, L. T.; Chang, L. C.; Chen, Y. L.; Huang, L. J.; Kuo, S. C.; Tzeng, C. C.; Lee, M. R.; Wang, J. P. *Biochem. Pharmacol.* **2007**, *73*, 1796.
18. Fang, K. C.; Chen, Y. L.; Sheu, J. Y.; Wang, T. C.; Tzeng, C. C. *J. Med. Chem.* **2000**, *43*, 3809.
19. Chen, Y. L.; Fang, K. C.; Sheu, J. Y.; Hsu, S. L.; Tzeng, C. C. *J. Med. Chem.* **2001**, *44*, 2374.
20. Tseng, C. H.; Tzeng, C. C.; Yang, C. L.; Lu, P. J.; Chen, H. L.; Li, H. Y.; Chuang, Y. C.; Yang, C. N.; Chen, Y. L. *J. Med. Chem.* **2010**, *53*, 6164.
21. Chen, Y. W.; Chen, Y. L.; Tseng, C. H.; Liang, C. C.; Yang, C. N.; Yao, Y. C.; Lu, P. J.; Tzeng, C. C. *J. Med. Chem.* **2011**, *54*, 4446.
22. Goldstein, H.; Radovanovitch, H. *Helv. Chim. Acta* **1926**, *9*, 783.
23. *The structure of* ***7a*** *was solved and refined by direct methods Shelx 97 (Sheldrick GM (1997) SHELXS 97, Program Crystal Structure Solution. University of Göttingen, Germany) suite of programs*: Orthorhombic, space group P 1 21/c 1, $a = 4.5317(3)$ Å, $b = 23.1087(12)$ Å, $c = 12.3031(7)$ Å, $\alpha = 90°$, $\beta = 99.531(4)°$, $\gamma = 90°$, $V = 1270.62(13)$ Å^3, $Z = 4$, δ (calcd) = 1.382 Mg m^{-3}, FW = 264.28 for $C_{16}H_{12}N_2O_2$, $F(000) = 552$. Complete crystallographic data for the structural analysis have been deposited with the Cambridge Crystallographic Data Centre, CCDC 881881 for compound **7a**. Copies of this information may be obtained free of charge from the Director, Cambridge Crystallographic Data Centre, 12 Union Road, Cambridge, CB2 1EZ, UK. (fax: +44-1223-336033, e-mail: deposit@ccdc.cam.ac.uk or via www.ccdc.cam.ac.uk).
24. Marcocci, L.; Maguire, J. J.; Droy-Lefaix, M. T.; Packer, L. *Biochem. Biophys. Res. Commun.* **1994**, *201*, 748.
25. Kim, H. G.; Shrestha, B.; Lim, S. Y.; Yoon, D. H.; Chang, W. C.; Shin, D. J.; Han, S. K.; Park, S. M.; Park, J. H.; Park, H. I.; Sung, J. M.; Jang, Y.; Chung, N.; Hwang, K. C.; Kim, T. W. *Eur. J. Pharmacol.* **2006**, *545*, 192.
26. Zhang, Y.; Dong, C. *Cell Mol. Life Sci.* **2007**, *64*, 2771.
27. Green, L. C.; Wagner, D. A.; Glogowski, J.; Skipper, P. L.; Wishnok, J. S.; Tannenbaum, S. R. *Anal. Biochem.* **1982**, *126*, 131.
28. Shalit, I.; Halperin, D.; Haite, D.; Levitov, A.; Romano, J.; Osherov, N.; Fabian, I. *J. Antimicrob. Chemother.* **2006**, *57*, 230.
29. Goodwin, C. J.; Holt, S. J.; Downes, S.; Marshall, N. J. *J. Immunol. Methods* **1995**, *179*, 95.
30. Bradford, M. M. *Anal. Biochem.* **1976**, *72*, 248.
31. Shin, K. M.; Kim, Y. H.; Park, W. S.; Kang, I.; Ha, J.; Choi, J. W.; Park, H. J.; Lee, K. T. *Biol. Pharm. Bull.* **2004**, *27*, 538.
32. Saja, K.; Babu, M. S.; Karunagaran, D.; Sudhakaran, P. R. *Int. Immunopharmacol.* **2007**, *7*, 1659.
33. Park, H. Y.; Han, M. H.; Park, C.; Jin, C. Y.; Kim, G. Y.; Choi, I. W.; Kim, N. D.; Nam, T. J.; Kwon, T. K.; Choi, Y. H. *Food Chem. Toxicol.* **2011**, *49*, 1745.